Eur. Phys. J. D (2014) 68: 165
DOI: 10.1140/epjd/e2014-40802-7

THE EUROPEAN PHYSICAL JOURNAL D

Regular Article

Brightness enhancement of a linac-based intense positron beam for total-reflection high-energy positron diffraction (TRHEPD)*

Masaki Maekawa[1], Ken Wada[2,a], Yuki Fukaya[1], Atsuo Kawasuso[1], Izumi Mochizuki[2], Tetsuo Shidara[3], and Toshio Hyodo[2]

[1] Advanced Science Research Center, Japan Atomic Energy Agency, 1233 Watanuki, Takasaki, Gunma 370-1292, Japan
[2] Institute of Materials Structure Science, High Energy Accelerator Research Organization (KEK), 1-1 Oho, Tsukuba, Ibaraki 305-0801, Japan
[3] Accelerator Laboratory, High Energy Accelerator Research Organization (KEK), 1-1 Oho, Tsukuba, Ibaraki 305-0801, Japan

Received 18 December 2013 / Received in final form 22 March 2014
Published online 27 June 2014 –

Abstract. The brightness of a linac-based intense positron beam was enhanced for total-reflection high-energy positron diffraction (TRHEPD) measurements. The beam initially guided by a magnetic field was released into a non-magnetic region and followed by a transmission-type remoderation. The term "TRHEPD" is a new name of reflection high-energy positron diffraction (RHEPD), which is a technique for the determination of the topmost- and near-surface atomic configurations; the total reflection of the positron beam from a solid surface is a unique superior characteristic. The present system provides the final beam of almost the same quality as the previous one with a ^{22}Na-based positron beam [A. Kawasuso et al., Rev. Sci. Instrum. **75**, 4585 (2004)] but much increased flux, i.e., almost the same emittance but much higher brightness. It gave a ∼60 times intensified diffraction pattern from a Si(111)–(7×7) reconstructed surface compared to the previous result. An improved signal-to-noise ratio in the obtained pattern due to the intensified beam allowed observation of clear fractional-order spots in the higher Laue-zones, which had not been observed previously.

1 Introduction

Reflection high-energy positron diffraction (RHEPD) [1], a positron counterpart of reflection high-energy electron diffraction (RHEED), is one of the ideal methods for solid-surface structure analysis. In contrast to the electron, the positron is totally reflected from the material surface when the glancing angle is smaller than a certain critical angle because of the positive crystal potential energy for the positron [1]. In a total reflection condition (e.g., $\leq 2^\circ$ for Si with 10-keV positrons), the positrons are reflected from the surface. We propose to rename this diffraction method as *total*-reflection high-energy positron diffraction (*TRHEPD*), emphasizing the advantage of the use of the total reflection.

In 1998, Kawasuso and Okada first succeeded in obtaining the TRHEPD (then called RHEPD) patterns from a hydrogen-terminated Si(111) surface by using a ^{22}Na-based electrostatic positron-beam apparatus at the Japan Atomic Energy Agency (JAEA), Takasaki [2]. In a subsequent work [3], Kawasuso et al. improved the quality of the beam by using magnetic lenses effectively to reduce the beam diameter. The final beam flux with the TRHEPD apparatus was 10^3–10^4 e^+/s, or 0.1–1 fA, which was extremely small compared with conventional RHEED apparatus, whose electron flux is typically ∼μA. Despite the small flux, this apparatus yielded various useful results from the specular spot analysis in determining the structures of metal-deposited surfaces of Si and Ge crystals [4], including determination of Si(111)–(8×2)–In surface structure at low temperature [5], and the details of the $\sqrt{21} \times \sqrt{21}$ structure of Ag deposited Si(111)–$(\sqrt{3} \times \sqrt{3})$ surface [6], both of which had not been determined with other surface structure analysis methods. These results proved that the TRHEPD is a very sensitive method for surface structure analysis.

The TRHEPD experiment is not easy to perform with a ^{22}Na-based beam because of the small beam flux; one has to accumulate on a PC positron signals on a micro-channel plate (MCP) with a phosphor screen and a CCD camera to check each sample azimuthal angle to find the correct one. Besides, fractional-order spots in higher-order Laue zones were not observed with such a beam because of the low signal-to-noise (S/N) ratio.

* Contribution to the Topical Issue "Electron and Positron Induced Processes", edited by Michael Brunger, Radu Campeanu, Masamitsu Hoshino, Oddur Ingólfsson, Paulo Limão-Vieira, Nigel Mason, Yasuyuki Nagashima and Hajime Tanuma.

[a] e-mail: ken.wada@kek.jp

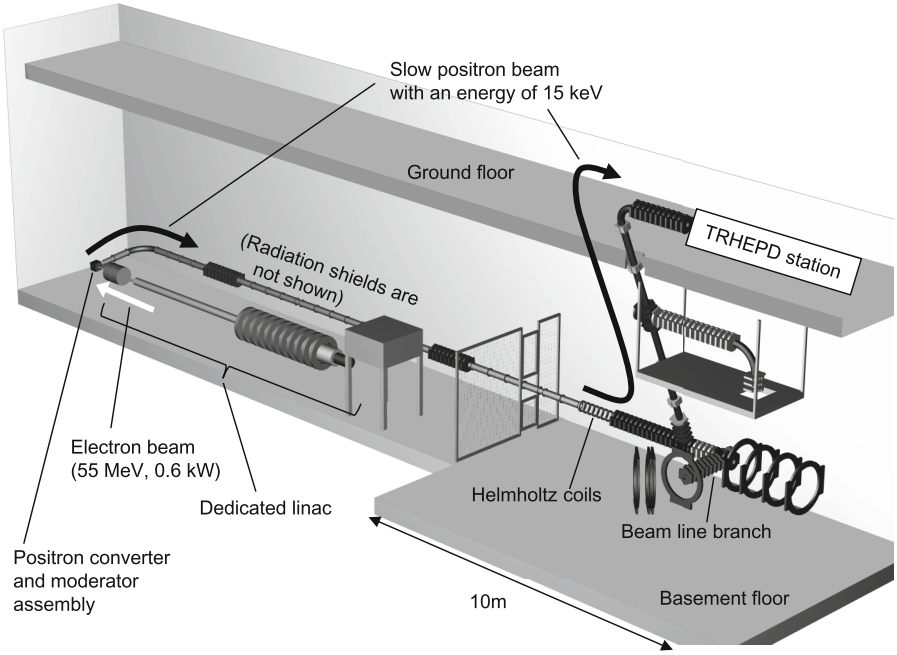

Fig. 1. Schematic view of the KEK Slow Positron Facility (as of June 2012) [8]. The positron beam generated by the dedicated linac and the positron converter/moderator assembly was guided by magnetic field from the basement floor to the TRHEPD station on the ground floor. (The station has been moved to the basement floor after this research.)

In the present study, we have utilized a high-intensity linac-based positron beam for TRHEPD experiments at the Slow Positron Facility, High Energy Accelerator Research Organization (KEK) [7,8]. It provides a few 10^7 slow-e^+/s, one or two orders of magnitude higher intensity than that of a ^{22}Na-based system.

2 TRHEPD experiment at KEK-SPF

Figure 1 shows a schematic view of the Slow Positron Facility (SPF) at KEK. A pulsed 50-Hz electron beam generated with a dedicated linac (operated at 55 MeV, 0.6 kW) is injected on a Ta converter and causes fast positron-electron pair creation through bremsstrahlung radiation. The positrons then shower down on 25 μm-thick W foils, are moderated (slow-downed) to thermal energy in the foils, and a fraction spontaneously comes out from the foil surfaces with an energy of 3 eV owing to the negative work function [7]. The positron converter/moderator assembly was held at an electrostatic voltage of 15 kV for TRHEPD. The emitted positrons were subsequently accelerated to 15 keV as they entered the grounded beam-line and were guided by the magnetic field of $\sim$0.015 T from the basement floor to the TRHEPD station on the ground floor.

For a diffraction experiment, positrons spirally transported by the magnetic field have to be first released into a non-magnetic region. Since the released positrons have large diameter, a brightness-enhancement unit should be effectively used to achieve a small-diameter and highly-parallel beam with a sufficient flux.

Figure 2 shows the brightness-enhancement unit and the TRHEPD chamber connected to a magnetic-transport beam-line. The beam was released into a non-magnetic region and was focused with a magnetic lens on a transmission-type remoderator (100-nm W film) [9–13]. The final magnetic coil of the beam-line produced reversed magnetic field to reduce the fringing field at the magnetic lens. An iron plate is placed near the final coil for the same purpose. The remoderator was annealed at $\sim$1200 °C for a few minutes by Joule heating before use. The 15-keV positron beam was incident on the remoderator at an electrostatic voltage of 10 kV; the 5 keV incident energy makes the maximum reemission efficiency for a 100-nm W foil [10]. Figure 3 shows results of a beam trajectory simulation, where the transport efficiency into the non-magnetic region was 55%. We have confirmed experimentally that the beam diameter was $\sim$1.5 mm in full-width-at-half-maximum (FWHM) by using a MCP-phosphor at the position of the remoderator.

The reemitted positrons were subsequently accelerated by four aperture electrodes (extractor, Wehnelt, Soa and anode) with a diameter of 7.5 mm and the spacing of 2.5 mm [3]. The beam was transported by four magnetic lenses and an objective lens, and was incident on a grounded sample. The beam transportation parameters were adjusted so that the beam was focused on the MCP assembly for the observation of the diffraction patterns.

A Si(111) sample was mounted on a sample holder driven by a five-axis PC-controlled manipulator in the TRHEPD experiment chamber. The sample surface was prepared by flash annealing to 1200 °C for a few seconds several times. The diffracted positrons were detected

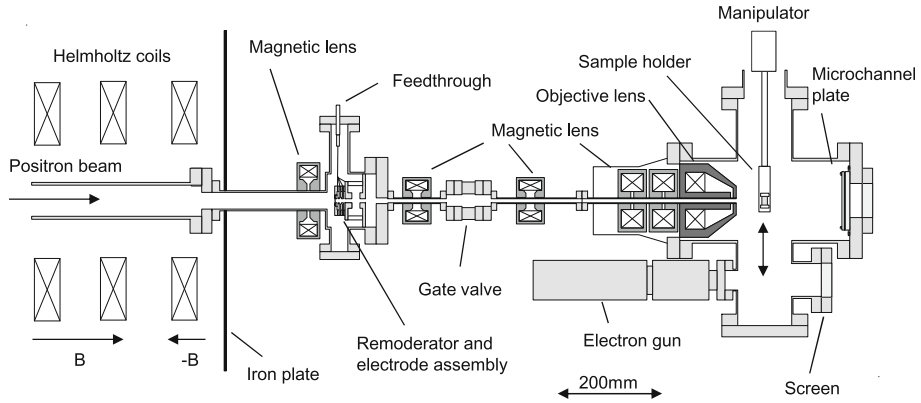

Fig. 2. The brightness-enhancement unit and the TRHEPD chamber connected to a KEK-SPF beam-line.

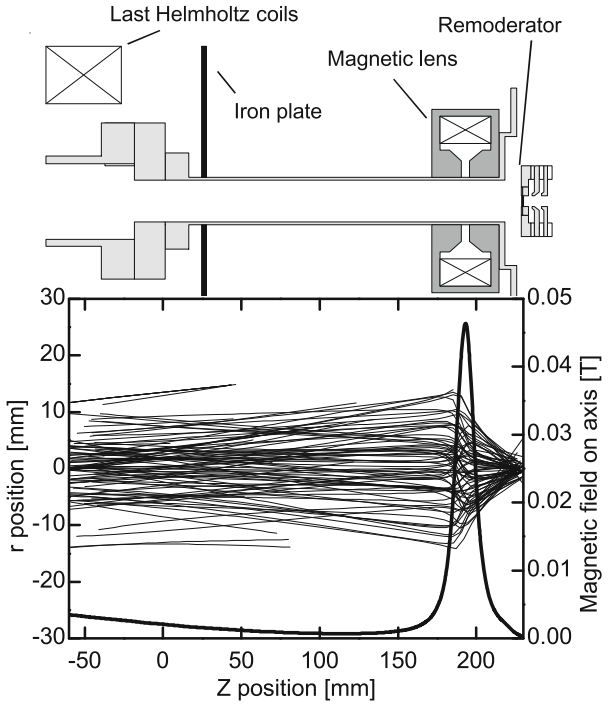

Fig. 3. A result of a beam trajectory simulation for magnetically transported positrons released into a non-magnetic region and focused on a remoderator by a magnetic lens.

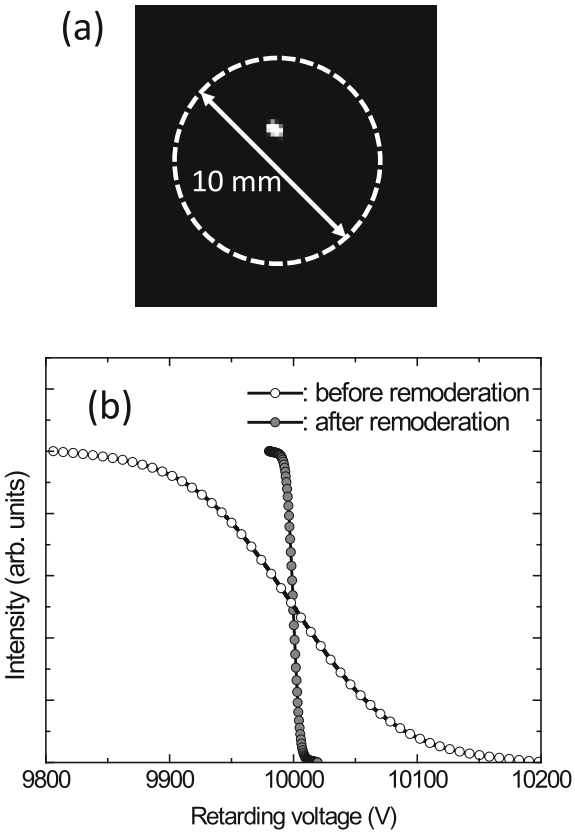

Fig. 4. (a) A typical image of a 10-keV positron beam after remoderation on a MCP-phosphor screen. (b) Intensities of the 10-keV positron beam before and after remoderation as a function of a longitudinal retarding voltage.

by a MCP-phosphor screen. The images of the diffraction patterns were accumulated by a CCD camera and a PC. A rocking curve (beam glancing angle dependence of the spot intensity) for the specular spot was measured. The base pressure of the TRHEPD chamber was less than 4×10^{-8} Pa.

3 Beam quality

Figure 4a shows a typical image of the remoderated positron beam at the sample position. The beam diameter is ∼0.5 mm (FWHM).

Figure 4b shows intensities of the positron beam before and after remoderation as a function of a longitudinal retarding voltage. The longitudinal energy-spread of the 10-keV beam was improved from 130 eV to 8 eV (FWHM) after the remoderation.

The beam brightness is defined as [14]

$$B = I/\varepsilon^2 E = I/r_{\mathrm{w}}^2 \theta_{\mathrm{HWHM}}^2 E, \qquad (1)$$

where I is the beam flux, E is the beam energy, r_{w} is the beam radius (the half-width-at-half-maximum (HWHM) diameter) at the beam waist, and θ_{HWHM} is the beam

divergence (HWHM). The beam emittance, ε, is defined as the area in particle position-angle plane occupied by beam particles divided by π.

Assuming the extraction efficiency into a non-magnetic region to be 50%, and the remoderation efficiency to be 10%, the final beam flux incident on the sample was estimated to be $\sim 10^6\,\mathrm{e}^+/\mathrm{s}$.

The brightness was estimated from the parameters of the reemitted positrons from the remoderator, $r_\mathrm{w} \sim 0.75$ mm, $\theta_\mathrm{HWHM} \sim 100$ mrad, and $E = 3$ eV, to be $B \sim 6 \times 10^9\ \mathrm{e}^+/\mathrm{s}/\mathrm{cm}^2/\mathrm{rad}^2/\mathrm{eV}$.

The brightness was also estimated from the emittance. The emittance is evaluated by measuring the beam size for various focusing powers of the objective lens. The beam radius R (HWHM of the beam diameter) at a distance L from the objective lens is expressed as:

$$R^2 = \beta\varepsilon L^2\left[1/f - (1/L - \alpha/\beta)\right]^2 + \varepsilon L^2/\beta^2 \qquad (2)$$

where α and β are the Twiss parameters [15], and f is the focal length of the objective lens. The value of f is given by [16]

$$f = \frac{d}{\sin\left(\pi/\sqrt{1+K}\right)}, \qquad (3)$$

$$K = \frac{e(Md)^2}{8m\Phi}. \qquad (4)$$

Here, e and m are the elemental charge and the electron rest mass, M is the magnetic flux density of the objective lens, d is the gap length of the lens (=2 mm), and Φ is the acceleration voltage of 10 kV. Figure 5a shows the observed R^2 against $1/f$. From fitting the quadratic function (2) to the data in Figure 5a, the emittance and the Twiss parameters were estimated and gave the corresponding phase diagram in the position-angle plane in Figure 5b. The estimated value of the emittance was 1.08 mm mrad.

From the values of I and ε estimated above, the brightness value with $E = 10$ keV was lead to be $B \sim 9 \times 10^9\,\mathrm{e}^+/\mathrm{s}/\mathrm{cm}^2/\mathrm{rad}^2/\mathrm{eV}$.

The brightness of the magnetically transported positrons was estimated to be $\sim 5 \times 10^6\ \mathrm{e}^+/\mathrm{s}/\mathrm{cm}^2/\mathrm{rad}^2/\mathrm{eV}$, with $r_\mathrm{w} \sim 10$ mm, $\theta_\mathrm{HWHM} \sim 50$ mrad, which is roughly estimated from the extraction efficiency into the non-magnetic region of 50% and the geometry, and $E = 15$ keV. Thus the present brightness-enhancement factor is 1000–2000.

The coherence length parallel to the beam direction, l_p, and the normal, l_n, are described as:

$$l_\mathrm{p} = 1\Bigg/\sqrt{\left(\frac{\Delta E}{24.5\sqrt{E}}\right)^2 + \left(\frac{\Delta\theta\sin\theta_\mathrm{g}}{\lambda}\right)^2} \quad (\text{in Å}) \qquad (5)$$

$$l_\mathrm{n} = \lambda/\Delta\theta \qquad (6)$$

where E and ΔE are the beam energy and its uncertainty (in eV), θ_g is the glancing angle, $\Delta\theta$ is the angular uncertainty, and λ is the wave length of the beam [17,18]. These coherence lengths are estimated to be $l_\mathrm{p} \sim 30$ nm and $l_\mathrm{n} \sim 1$ nm, respectively, when $E = 10$ keV, $\Delta E \sim 40$ meV (thermal energy at 300 K), $\Delta\theta = 12$ mrad, and $\theta_\mathrm{g} = 2°$. The value of l_p is greater than the relatively large unit cell of the 7×7 reconstructed structure of the Si(111) surface. The value of l_n corresponds to a distance of a few atomic layers, which is sufficient for the TRHEPD experiment.

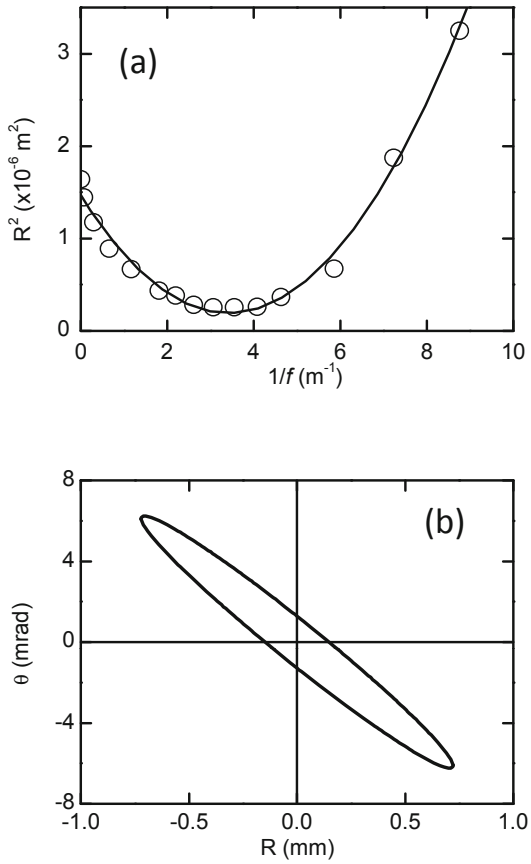

Fig. 5. (a) Beam size versus focusing power of the objective lens. (b) The phase diagram of the positrons in the position-angle plane.

4 Diffraction patterns

Figure 6a shows a diffraction pattern for a glancing angle of 2.1° (>critical angle, 2.0°) from a Si(111)–(7 × 7) surface observed with the brightness-enhanced linac-based 10-keV beam developed in this study, and Figure 6b that for the same angle observed with the ^{22}Na-based system previously reported [3]. Figure 7a shows the rocking curves of the specular spot normalized by the measurement time observed with the present linac-based beam, and that with ^{22}Na-based system in the previous work. Note that the ^{22}Na data are multiplied by 10 for the sake of visibility. The diffraction intensity with the linac-based beam has been about 60 times intensified compared to that with the ^{22}Na-based.

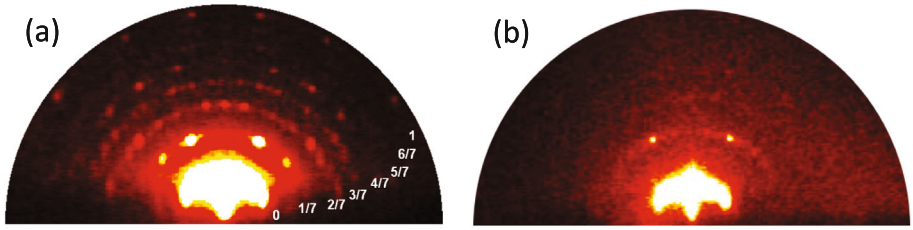

Fig. 6. (a) A diffraction pattern for a glancing angle of 2.1° (> critical angle, 2.0°) from a Si(111)–(7×7) surface observed with the remoderated linac-based 10-keV positron beam [19,20], and (b) that for the same angle observed with a ^{22}Na-based beam.

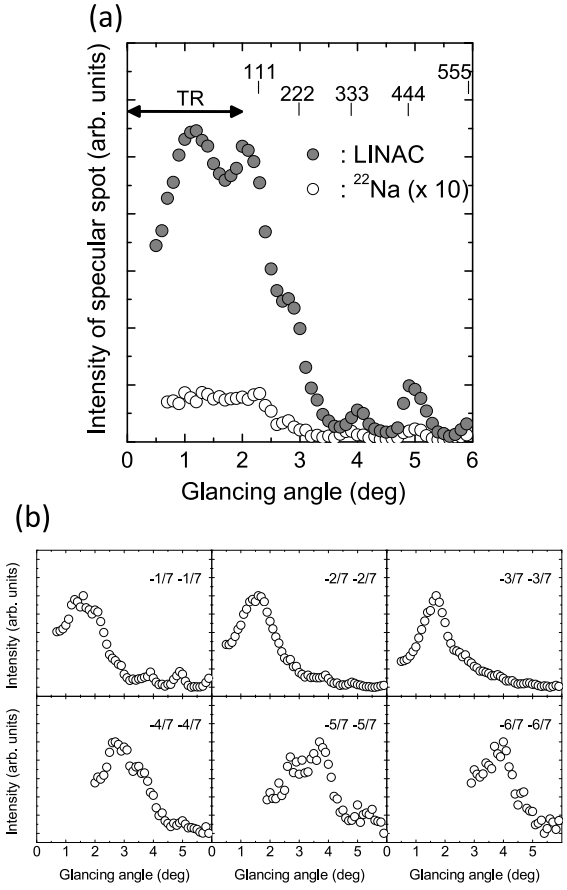

Fig. 7. (a) TRHEPD rocking curves of specular spots from a Si(111)–(7×7) surface. The closed and open circles denote the rocking curves observed by using the linac- and ^{22}Na-based positron beams, respectively. The ^{22}Na data are multiplied by 10 for the sake of visibility. "TR" stands for the total-reflection region. The indices of the Bragg reflection are labeled on the top of the figure. (b) Rocking curves of fractional-order spots from the Si(111)–(7×7) surface observed with the linac-based system.

It is interesting to note that the emittance of the present beam is about the same as the previous one [3][1], so that the difference in the brightness is predominantly attributed to the increase in the intensity of the final beam used for the TRHEPD measurements. The previous beam used a ^{22}Na positron source with an active diameter of 5 mm, electrostatic transport, and apertures, while the present beam uses a converter/moderator assembly with an active diameter of ∼20 mm, magnetic transport, and a transmission-type remoderator. Roughly speaking, because of the lower quality of the present initial beam, large loss of the intensity was inevitable to obtain the same emittance as the previous one, but the much higher initial intensity makes it possible to keep the final intensity higher, which directly contributes the 60–90 times higher brightness.

The much intensified beam with the present system has allowed adjustment of the sample azimuthal angle without accumulating the positron signals. It took about three hours to obtain one rocking curve plotted by the closed circles shown in Figure 7a, and about one hour for the diffraction pattern shown in Figure 6a.

The fractional-order spots in higher Laue-zones, which are hard to be recognized in a previous result (Fig. 6b), has been observed clearly in the present study as shown in Figure 6a owing to the much intensified beam flux. The primary origins of the backgrounds in the MCP-phosphor images are electrons emitted from a RHEED gun used for the sample preparation and remaining warm during the measurements in UHV, and the dark currents of the MCPs. A commercial-grade CCD camera and capture-board system used for the diffraction pattern observations also caused a part of the noises. Figure 7b shows the present rocking curves of the fractional-order spots, the higher order ones of which are only possible to observe with the present beam. Despite the use of essentially the same detection system, it is evident that the shortening of the measurement time has contributed significantly to the improvement of the S/N ratio.

With the present system, it has been demonstrated that the TRHEPD pattern from a Si(111)–(7 × 7) reconstructed surface for the total reflection condition does not contain contributions from atoms in the bulk [19,20]. We have also determined the detailed structure of silicene on a Ag(111) surface with this system [21].

5 Conclusion

A high-intensity linac-based positron beam with an energy of 15 keV has been remoderated to be 10-keV brightness-enhanced beam for TRHEPD experiments.

[1] The brightness value of $\sim 10^7 e^+/s/cm^2/rad^2/eV$ in the article [3] is multiplide by π^2 in this paper to adjust the difference in the definitions of emittance by a factor of π.

The present system achieved a brightness enhancement of 1000–2000 times from the magnetically guided beam to the low-emittance beam. The intensity of the specular spot from a Si(111)–(7×7) reconstructed surface observed by the present beam was found to be about 60 times higher than that observed by using the previous ^{22}Na-based beam. The emittance of the final beam with the present system is almost the same as the previous one but the brightness is much higher owing to the higher intensity of the beam. An improved signal-to-noise ratio in the diffraction pattern due to the intensified beam flux allowed clear observation of fractional-order spots in the higher Laue-zones.

This research was conducted under the PF Proposal No. 2012G653 and the auspices of the Joint Development Research at the High Energy Accelerator Research Organization (KEK). The present work was partly supported by a Grant-in-Aid for Scientific Research, Grant No. (S) 24221007, from JSPS.

References

1. A. Ichimiya, Solid State Phenom. **28-29**, 143 (1992)
2. A. Kawasuso, S. Okada, Phys. Rev. Lett. **81**, 2695 (1998)
3. A. Kawasuso, T. Ishimoto, M. Maekawa, Y. Fukaya, K. Hayashi, A. Ichimiya, Rev. Sci. Instrum. **75**, 4585 (2004)
4. Y. Fukaya, M. Maekawa, I. Mochizuki, K. Wada, T. Hyodo, A. Kawasuso, J. Phys.: Conf. Ser. **443**, 012068 (2013)
5. Y. Fukaya, M. Hashimoto, A. Kawasuso, A. Ichimiya, Surf. Sci. **602**, 2448 (2008)
6. Y. Fukaya, A. Kawasuso, A. Ichimiya, Surf. Sci. **601**, 5187 (2007)
7. K. Wada, T. Hyodo, A. Yagishita, M. Ikeda, S. Ohsawa, T. Shidara, K. Michishio, T. Tachibana, Y. Nagashima, Y. Fukaya, M. Maekawa, A. Kawasuso, Eur. Phys. J. D **66**, 37 (2012)
8. K. Wada, T. Hyodo, T. Kosuge, Y. Saito, M. Ikeda, S. Ohsawa, T. Shidara, K. Michishio, T. Tachibana, H. Terabe, R.H. Suzuki, Y. Nagashima, Y. Fukaya, M. Maekawa, I. Mochizuki, A. Kawasuso, J. Phys.: Conf. Ser. **443**, 012082 (2013)
9. A.P. Mills Jr., R.J. Wilson, Phys. Rev. A **26**, 490 (1982)
10. D.M. Chen, K.G. Lynn, R. Pareja, B. Nielsen, Phys. Rev. B **31**, 4123 (1985)
11. F.M. Jacobsen, M. Charlton, J. Chevallier, B.I. Deutch, G. Laricchia, M.R. Poulsen, J. Appl. Phys. **67**, 575 (1990)
12. N. Oshima, R. Suzuki, T. Ohdaira, A. Kinomura, T. Narumi, A. Uedono, M. Fujinami, J. Appl. Phys. **103**, 094916 (2008)
13. M. Fujinami, S. Jinno, M. Fukuzumi, T. Kawaguchi, K. Oguma, T. Akahane, Anal. Sci. **24**, 73 (2008)
14. A.P. Mills Jr., Appl. Phys. **23**, 189 (1980)
15. H. Wollnik, *Optics of Charged Particle* (Academic, New York, 1987), p. 151
16. K.R. Spangenberg, *Vacuum Tubes* (McGraw-Hill Book Company Inc., 1948), p. 402
17. G. Comsa, Surf. Sci. **81**, 57 (1979)
18. A. Ichimiya, *Reflection High Energy Electron Diffraction* (Cambridge University Press, New York, 2004), p. 107
19. Y. Fukaya, M. Maekawa, A. Kawasuso, I. Mochizuki, K. Wada, T. Shidara, A. Ichimiya, T. Hyodo, Appl. Phys. Express **7**, 056601 (2014)
20. T. Hyodo, Y. Fukaya, M. Maekawa, I. Mochizuki, K. Wada, T. Shidara, A. Ichimiya, A. Kawasuso, J. Phys.: Conf. Ser. **505**, 012001 (2014)
21. Y. Fukaya, I. Mochizuki, M. Maekawa, K. Wada, T. Hyodo, I. Matsuda, A. Kawasuso, Phys. Rev. B **88**, 205413 (2013)